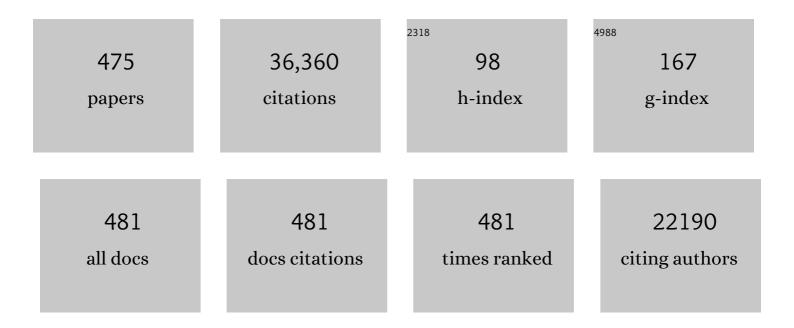
List of Publications by Year in descending order

Source: https://exaly.com/author-pdf/5429361/publications.pdf Version: 2024-02-01



#	Article	IF	CITATIONS
1	Green antisolvent additive engineering to improve the performance of perovskite solar cells. Journal of Energy Chemistry, 2022, 66, 1-8.	7.1	42
2	Double Side Interfacial Optimization for Lowâ€Temperature Stable CsPbI <sub>2</sub> Br Perovskite Solar Cells with High Efficiency Beyond 16%. Energy and Environmental Materials, 2022, 5, 637-644.	7.3	27
3	Post-treatment by an ionic tetrabutylammonium hexafluorophosphate for improved efficiency and stability of perovskite solar cells. Journal of Energy Chemistry, 2022, 64, 8-15.	7.1	19
4	Lead-free molecular one-dimensional perovskite for efficient X-ray detection. Journal of Energy Chemistry, 2022, 64, 209-213.	7.1	15
5	Graded 2D/3D (CF3-PEA)2FA0.85MA0.15Pb2I7/FA0.85MA0.15PbI3 heterojunction for stable perovskite solar cell with an efficiency over 23.0%. Journal of Energy Chemistry, 2022, 65, 480-489.	7.1	34
6	Spontaneous Construction of Multidimensional Heterostructure Enables Enhanced Hole Extraction for Inorganic Perovskite Solar Cells to Exceed 20% Efficiency. Advanced Energy Materials, 2022, 12, 2103007.	10.2	42
7	Ionâ€Accumulationâ€Induced Charge Tunneling for High Gain Factor in P–I–Nâ€Structured Perovskite CH <sub>3</sub> NH <sub>3</sub> PbI <sub>3</sub> Xâ€Ray Detector. Advanced Materials Technologies, 2022, 7, 2100908.	3.0	15
8	Unraveling Passivation Mechanism of Imidazolium-Based Ionic Liquids on Inorganic Perovskite to Achieve Near-Record-Efficiency CsPbI2Br Solar Cells. Nano-Micro Letters, 2022, 14, 7.	14.4	58
9	A Key 2D Intermediate Phase for Stable Highâ€Efficiency CsPbI <sub>2</sub> Br Perovskite Solar Cells. Advanced Energy Materials, 2022, 12, 2103019.	10.2	44
10	Perovskite Quantum Dots in Solar Cells. Advanced Science, 2022, 9, e2104577.	5.6	49
11	Formamidinium-based Ruddlesden–Popper perovskite films fabricated <i>via</i> two-step sequential deposition: quantum well formation, physical properties and film-based solar cells. Energy and Environmental Science, 2022, 15, 1144-1155.	15.6	27
12	Diaminobenzene Dihydroiodideâ€MA <sub>0.6</sub> FA <sub>0.4</sub> PbI <sub>3â^'</sub> <i><sub>x</sub></i> Cl <i><sub>xUnsymmetrical Perovskites with over 22% Efficiency for High Stability Solar Cells. Advanced Functional Materials, 2022, 32, .</sub></i>	b≥<∕i> 7.8	16
13	Rational Design of Heterojunction Interface for Cu <sub>2</sub> ZnSn(S,Se) <sub>4</sub> Solar Cells to Exceed 12% Efficiency. Solar Rrl, 2022, 6, .	3.1	15
14	Highly Efficient and Stable CsPbTh <sub>3</sub> (Th = I, Br, Cl) Perovskite Solar Cells by Combinational Passivation Strategy. Advanced Science, 2022, 9, e2105103.	5.6	20
15	Ionic Liquid Treatment for Highestâ€Efficiency Ambient Printed Stable Allâ€Inorganic CsPbI <sub>3</sub> Perovskite Solar Cells. Advanced Materials, 2022, 34, e2106750.	11.1	97
16	2D-C <sub>3</sub> N <sub>4</sub> encapsulated perovskite nanocrystals for efficient photo-assisted thermocatalytic CO <sub>2</sub> reduction. Chemical Science, 2022, 13, 1335-1341.	3.7	29
17	All-Inorganic Perovskite Solar Cells with Tetrabutylammonium Acetate as the Buffer Layer between the SnO <sub>2</sub> Electron Transport Film and CsPbI <sub>3</sub> . ACS Applied Materials & Interfaces, 2022, 14, 5183-5193.	4.0	20
18	Centimeter-Sized 2D Perovskitoid Single Crystals for Efficient X-ray Photoresponsivity. Chemistry of Materials, 2022, 34, 1699-1709.	3.2	24

#	Article	IF	CITATIONS
19	Unveiling the effect of interstitial dopants on CO2 activation over CsPbBr3 catalyst for efficient photothermal CO2 reduction. Chemical Engineering Journal, 2022, 435, 135071.	6.6	35
20	Imidazolium-based ionic liquid for stable and highly efficient black-phase formamidinium-based perovskite solar cell. Chemical Engineering Journal, 2022, 434, 134759.	6.6	5
21	Surface reconstruction strategy improves the all-inorganic CsPbIBr2 based perovskite solar cells and photodetectors performance. Nano Energy, 2022, 94, 106960.	8.2	35
22	Polarity regulation for stable 2D-perovskite-encapsulated high-efficiency 3D-perovskite solar cells. Nano Energy, 2022, 95, 106965.	8.2	27
23	Symmetrical Acceptor–Donor–Acceptor Molecule as a Versatile Defect Passivation Agent toward Efficient FA <sub>0.85</sub> MA <sub>0.15</sub> PbI <sub>3</sub> Perovskite Solar Cells. Advanced Functional Materials, 2022, 32, .	7.8	47
24	Inch-size Cs <sub>3</sub> Bi <sub>2</sub> I <sub>9</sub> polycrystalline wafers with near-intrinsic properties for ultralow-detection-limit X-ray detection. Journal of Materials Chemistry C, 2022, 10, 6665-6672.	2.7	18
25	Intermediate phase engineering of halide perovskites for photovoltaics. Joule, 2022, 6, 315-339.	11.7	60
26	Recent Developments in Upscalable Printing Techniques for Perovskite Solar Cells. Advanced Science, 2022, 9, e2200308.	5.6	40
27	Utilizing the Energy Transfer of Ce <sup>4+</sup> – and Ce <sup>3+</sup> –Tb <sup>3+</sup> to Boost the Luminescence Quantum Efficiency up to 100% in Borate Glass. Journal of Physical Chemistry C, 2022, 126, 5838-5846.	1.5	3
28	Protonâ€transferâ€induced in situ defect passivation for highly efficient wideâ€bandgap inverted perovskite solar cells. InformaÄnÃ-Materiály, 2022, 4, .	8.5	27
29	Wideâ€Bandgap Organic–Inorganic Lead Halide Perovskite Solar Cells. Advanced Science, 2022, 9, e2105085.	5.6	60
30	Carrier Generation Engineering toward 18% Efficiency Organic Solar Cells by Controlling Film Microstructure. Advanced Energy Materials, 2022, 12, .	10.2	25
31	Ligandâ€Anchoringâ€Induced Oriented Crystal Growth for Highâ€Efficiency Leadâ€Tin Perovskite Solar Cells. Advanced Functional Materials, 2022, 32, .	7.8	38
32	Firstâ€Principles Calculation Design for 2D Perovskite to Suppress Ion Migration for Highâ€Performance Xâ€ray Detection. Advanced Functional Materials, 2022, 32, .	7.8	36
33	In Situ Study of Molecular Aggregation in Conjugated Polymer/Elastomer Blends toward Stretchable Electronics. Macromolecules, 2022, 55, 297-308.	2.2	30
34	lonicâ€Liquidâ€Perovskite Capping Layer for Stable 24.33%â€Efficient Solar Cell. Advanced Energy Materials, 2022, 12, .	10.2	80
35	Recordâ€Efficiency Flexible Perovskite Solar Cells Enabled by Multifunctional Organic Ions Interface Passivation. Advanced Materials, 2022, 34, e2201681.	11.1	186
36	Amino Acidâ€Based Lowâ€Dimensional Management for Enhanced Perovskite Solar Cells. Solar Rrl, 2022, 6,	3.1	3

#	Article	IF	CITATIONS
37	Recent Progress of Electrode Materials for Flexible Perovskite Solar Cells. Nano-Micro Letters, 2022, 14, 117.	14.4	68
38	4â€Hydrazinobenzoicâ€Acid Antioxidant for Highâ€Efficiency Sn–Pb Alloyed Perovskite Solar Cells. Energy Technology, 2022, 10, .	1.8	10
39	Waterâ€Resistant Leadâ€Free Perovskitoid Single Crystal for Efficient Xâ€Ray Detection. Advanced Functional Materials, 2022, 32, .	7.8	18
40	Flexible perovskite solar cells: Material selection and structure design. Applied Physics Reviews, 2022, 9, .	5.5	19
41	Enhanced visible-light photocatalytic activity of hydrogenated Fe3O4 nanooctahedrons with {111} polar facets in degradation of Basic Fuchsin and the photocatalytic mechanism. Journal of Materials Science: Materials in Electronics, 2022, 33, 13095-13109.	1.1	1
42	Alkyl Diamine-Induced (100)-Preferred Crystal Orientation for Efficient Pb–Sn Perovskite Solar Cells. ACS Applied Energy Materials, 2022, 5, 6936-6942.	2.5	12
43	Structural and Functional Insights into Metal-Free Perovskites. Journal of Physical Chemistry Letters, 2022, 13, 5168-5178.	2.1	8
44	Collaborative Strategy of Multifunctional Groups in Trifluoroacetamide Achieving Efficient and Stable Perovskite Solar Cells. Solar Rrl, 2022, 6, .	3.1	17
45	Hydrazide Derivatives for Defect Passivation in Pure CsPbI <sub>3</sub> Perovskite Solar Cells. Angewandte Chemie - International Edition, 2022, 61, .	7.2	95
46	Stable Highâ€Efficiency CsPbI <sub>2</sub> Br Solar Cells by Designed Passivation Using Multifunctional 2D Perovskite. Advanced Functional Materials, 2022, 32, .	7.8	27
47	Stable 24.29%â€Efficiency FA <sub>0.85</sub> MA <sub>0.15</sub> PbI <sub>3</sub> Perovskite Solar Cells Enabled by Methyl Haloacetate‣ead Dimer Complex. Advanced Energy Materials, 2022, 12, .	10.2	54
48	In-situ photoisomerization of azobenzene to inhibit ion-migration for stable high-efficiency perovskite solar cells. Journal of Energy Chemistry, 2022, 73, 556-564.	7.1	7
49	Effect of Solvent Residue in the Thin-Film Fabrication on Perovskite Solar Cell Performance. ACS Applied Materials & Interfaces, 2022, 14, 28729-28737.	4.0	22
50	Synergetic surface defect passivation towards efficient and stable inorganic perovskite solar cells. Chemical Engineering Journal, 2022, 447, 137515.	6.6	24
51	Powering the World with Solar Fuels from Photoelectrochemical CO <sub>2</sub> Reduction: Basic Principles and Recent Advances. Advanced Energy Materials, 2022, 12, .	10.2	44
52	Roles of Organic Ligands in Ambient Stability of Layered Halide Perovskites. ACS Applied Materials & Interfaces, 2022, 14, 33085-33093.	4.0	2
53	Balanced-Strength Additive for High-Efficiency Stable Perovskite Solar Cells. ACS Applied Energy Materials, 2022, 5, 8034-8041.	2.5	10
54	Synergistic Crystallization and Passivation by a Single Molecular Additive for Highâ€Performance Perovskite Solar Cells. Advanced Materials, 2022, 34, .	11.1	37

#	Article	IF	CITATIONS
55	Efficient Eco-Friendly Flexible X-ray Detectors Based on Molecular Perovskite. Nano Letters, 2022, 22, 5973-5981.	4.5	19
56	First observation of magnon transport in organic-inorganic hybrid perovskite. Matter, 2022, , .	5.0	4
57	Synergistic Effect of Antiâ€Solvent and Component Engineering for Effective Passivation to Attain Highly Stable Perovskite Solar Cells. Solar Rrl, 2022, 6, .	3.1	15
58	Metal-doped Mo2C (metal = Fe, Co, Ni, Cu) as catalysts on TiO2 for photocatalytic hydrogen evolution in neutral solution. Chinese Journal of Catalysis, 2021, 42, 205-216.	6.9	64
59	Multifunctional Enhancement for Highly Stable and Efficient Perovskite Solar Cells. Advanced Functional Materials, 2021, 31, 2005776.	7.8	273
60	Highâ€Efficiency Perovskite Solar Cells with Imidazoliumâ€Based Ionic Liquid for Surface Passivation and Charge Transport. Angewandte Chemie - International Edition, 2021, 60, 4238-4244.	7.2	221
61	Sequential Formation of Tunableâ€Bandgap Mixedâ€Halide Leadâ€Based Perovskites: In Situ Investigation and Photovoltaic Devices. Solar Rrl, 2021, 5, .	3.1	15
62	Hot Debate on Perovskite Solar Cells: Stability, Toxicity, High-Efficiency and Low Cost. Journal of Energy Chemistry, 2021, 53, 407-411.	7.1	9
63	Superior photovoltaics/optoelectronics of two-dimensional halide perovskites. Journal of Energy Chemistry, 2021, 57, 69-82.	7.1	20
64	ASnX <sub>3</sub> —Better than Pbâ€based Perovskite. Nano Select, 2021, 2, 159-186.	1.9	5
65	Recent advances in resistive random access memory based on lead halide perovskite. InformaÄnÃ- Materiály, 2021, 3, 293-315.	8.5	70
66	Breaking Platinum Nanoparticles to Singleâ€Atomic Ptâ€C <sub>4</sub> Coâ€catalysts for Enhanced Solarâ€toâ€Hydrogen Conversion. Angewandte Chemie - International Edition, 2021, 60, 2541-2547.	7.2	51
67	Self-assembled CoOOH on TiO2 for enhanced photoelectrochemical water oxidation. Journal of Energy Chemistry, 2021, 60, 512-521.	7.1	20
68	Synergistically Enhanced Amplified Spontaneous Emission by Cd Doping and Clâ€Assisted Crystallization. Advanced Optical Materials, 2021, 9, 2001825.	3.6	2
69	Breaking Platinum Nanoparticles to Singleâ€Atomic Ptâ€C 4 Coâ€catalysts for Enhanced Solarâ€toâ€Hydrogen Conversion. Angewandte Chemie, 2021, 133, 2571-2577.	1.6	8
70	Improving Performance and Stability of Planar Perovskite Solar Cells Through Passivation Effect with Green Additives. Solar Rrl, 2021, 5, 2000732.	3.1	5
71	Highâ€Efficiency Perovskite Solar Cells with Imidazoliumâ€Based Ionic Liquid for Surface Passivation and Charge Transport. Angewandte Chemie, 2021, 133, 4284-4290.	1.6	14
72	High Density and Unit Activity Integrated in Amorphous Catalysts for Electrochemical Water Splitting. Small Structures, 2021, 2, 2000096.	6.9	102

#	Article	IF	CITATIONS
73	Nanoconfined Crystallization for Highâ€Efficiency Inorganic Perovskite Solar Cells. Small Science, 2021, 1, 2000054.	5.8	19
74	Stability of the CsPbI <sub>3</sub> perovskite: from fundamentals to improvements. Journal of Materials Chemistry A, 2021, 9, 11124-11144.	5.2	78
75	High-efficiency and thermal/moisture stable CsPbI <sub>2.84</sub> Br <sub>0.16</sub> inorganic perovskite solar cells enabled by a multifunctional cesium trimethylacetate organic additive. Journal of Materials Chemistry A, 2021, 9, 4922-4932.	5.2	12
76	Microstructure and lattice strain control towards high-performance ambient green-printed perovskite solar cells. Journal of Materials Chemistry A, 2021, 9, 13297-13305.	5.2	29
77	High-throughput large-area vacuum deposition for high-performance formamidine-based perovskite solar cells. Energy and Environmental Science, 2021, 14, 3035-3043.	15.6	121
78	Unraveling the crucial role of spacer ligands in tuning the contact properties of metal–2D perovskite interfaces. Journal of Materials Chemistry C, 2021, 9, 8489-8495.	2.7	3
79	Metalâ€Free Organic Halide Perovskite: A New Class for Next Optoelectronic Generation Devices. Advanced Energy Materials, 2021, 11, 2003331.	10.2	29
80	Tripleâ€Cation and Mixedâ€Halide Perovskite Single Crystal for Highâ€Performance Xâ€ray Imaging. Advanced Materials, 2021, 33, e2006010.	11.1	163
81	Dualâ€Interface Modification of CsPbIBr <sub>2</sub> Solar Cells with Improved Efficiency and Stability. Advanced Materials Interfaces, 2021, 8, 2001994.	1.9	12
82	Molecular Engineering for Two-Dimensional Perovskites with Photovoltaic Efficiency Exceeding 18%. Matter, 2021, 4, 582-599.	5.0	123
83	Perovskite Solar Cells toward Eco-Friendly Printing. Research, 2021, 2021, 9671892.	2.8	18
84	Inch-sized high-quality perovskite single crystals by suppressing phase segregation for light-powered integrated circuits. Science Advances, 2021, 7, .	4.7	81
85	Defect Engineering in Earthâ€Abundant Cu <sub>2</sub> ZnSn(S,Se) <sub>4</sub> Photovoltaic Materials via Ga <sup>3+</sup> â€Doping for over 12% Efficient Solar Cells. Advanced Functional Materials, 2021, 31, 2010325.	7.8	79
86	van der Waals Interaction-Induced Tunable Schottky Barriers in Metal–2D Perovskite Contacts. Journal of Physical Chemistry Letters, 2021, 12, 1718-1725.	2.1	11
87	Dual interfacial engineering for efficient Cs2AgBiBr6 based solar cells. Journal of Energy Chemistry, 2021, 53, 372-378.	7.1	46
88	Centimeter‣ized Molecular Perovskite Crystal for Efficient Xâ€Ray Detection. Advanced Functional Materials, 2021, 31, 2100691.	7.8	22
89	Photogenerated Charge Separation between Polar Crystal Facets Under a Spontaneous Electric Field. Advanced Optical Materials, 2021, 9, 2001898.	3.6	7
90	Film Formation Control for High Performance Dion–Jacobson 2D Perovskite Solar Cells. Advanced Energy Materials, 2021, 11, 2002733.	10.2	62

#	Article	IF	CITATIONS
91	In‧itu Hot Oxygen Cleansing and Passivation for Allâ€Inorganic Perovskite Solar Cells Deposited in Ambient to Breakthrough 19% Efficiency. Advanced Functional Materials, 2021, 31, 2101568.	7.8	42
92	Hole‧torage Enhanced a‧i Photocathodes for Efficient Hydrogen Production. Angewandte Chemie, 2021, 133, 12073-12079.	1.6	2
93	Holeâ€Storage Enhanced aâ€Si Photocathodes for Efficient Hydrogen Production. Angewandte Chemie - International Edition, 2021, 60, 11966-11972.	7.2	29
94	Versatile Bidentate Chemical Passivation on a Cesium Lead Inorganic Perovskite for Efficient and Stable Photovoltaics. ACS Applied Energy Materials, 2021, 4, 4021-4028.	2.5	16
95	Simultaneous dual-interface and bulk defect passivation for high-efficiency and stable CsPbI2Br perovskite solar cells. Journal of Power Sources, 2021, 492, 229580.	4.0	13
96	Synergistic Effect of RbBr Interface Modification on Highly Efficient and Stable Perovskite Solar Cells. ACS Omega, 2021, 6, 13766-13773.	1.6	3
97	Enhanced Efficiency of Inorganic CsPbI <sub>3â^'</sub> <i><sub>x</sub></i> Br <i><sub>x</sub></i> Perovskite Solar Cell via Selfâ€Regulation of Antisite Defects. Advanced Energy Materials, 2021, 11, 2100403.	10.2	45
98	40.1% Record Lowâ€Light Solarâ€Cell Efficiency by Holistic Trapâ€Passivation using Micrometerâ€Thick Perovskite Film. Advanced Materials, 2021, 33, e2100770.	11.1	110
99	Effective Phaseâ€Alignment for 2D Halide Perovskites Incorporating Symmetric Diammonium Ion for Photovoltaics. Advanced Science, 2021, 8, e2001433.	5.6	32
100	Stable 2D Alternating Cation Perovskite Solar Cells with Power Conversion Efficiency >19% via Solvent Engineering. Solar Rrl, 2021, 5, 2100286.	3.1	45
101	Antisolvent―and Annealingâ€Free Deposition for Highly Stable Efficient Perovskite Solar Cells via Modified ZnO. Advanced Science, 2021, 8, 2002860.	5.6	47
102	Semitransparent Flexible Perovskite Solar Cells for Potential Greenhouse Applications. Solar Rrl, 2021, 5, 2100264.	3.1	15
103	Samariumâ€Doped Nickel Oxide for Superior Inverted Perovskite Solar Cells: Insight into Doping Effect for Electronic Applications. Advanced Functional Materials, 2021, 31, 2102452.	7.8	41
104	Enhanced Efficiency and Stability of Allâ€Inorganic CsPbI <sub>2</sub> Br Perovskite Solar Cells by Organic and Ionic Mixed Passivation. Advanced Science, 2021, 8, e2101367.	5.6	66
105	Tapered Coaxial Arrays for Photon―and Plasmonâ€Enhanced Light Harvesting in Perovskite Solar Cells: A Theoretical Investigation Using the Finite Element Method. ChemPlusChem, 2021, 86, 858-864.	1.3	5
106	28.3%-efficiency perovskite/silicon tandem solar cell by optimal transparent electrode for high efficient semitransparent top cell. Nano Energy, 2021, 84, 105934.	8.2	93
107	Deepâ€Level Transient Spectroscopy for Effective Passivator Selection in Perovskite Solar Cells to Attain High Efficiency over 23%. ChemSusChem, 2021, 14, 3182-3189.	3.6	24
108	Fluoroethylamine Engineering for Effective Passivation to Attain 23.4% Efficiency Perovskite Solar Cells with Superior Stability. Advanced Energy Materials, 2021, 11, 2101454.	10.2	49

#	Article	IF	CITATIONS
109	Flexible perovskite solar cells with simultaneously improved efficiency, operational stability, and mechanical reliability. Joule, 2021, 5, 1587-1601.	11.7	120
110	Cation Engineering for Effective Defect Passivation to Improve Efficiency and Stability of FA0.5MA0.5PbI3 Perovskite Solar Cells. ACS Applied Energy Materials, 2021, 4, 7654-7660.	2.5	3
111	Highly Luminescent Metalâ€Free Perovskite Single Crystal for Biocompatible Xâ€Ray Detector to Attain Highest Sensitivity. Advanced Materials, 2021, 33, e2102190.	11.1	46
112	Singleâ€Atom Doping and Highâ€Valence State for Synergistic Enhancement of NiO Electrocatalytic Water Oxidation. Small, 2021, 17, e2102448.	5.2	28
113	Halide-modulated self-assembly of metal-free perovskite single crystals for bio-friendly X-ray detection. Matter, 2021, 4, 2490-2507.	5.0	47
114	Enabling Solar Hydrogen Production over Selenium: Surface State Passivation and Cocatalyst Decoration. ACS Sustainable Chemistry and Engineering, 2021, 9, 9923-9931.	3.2	7
115	Room-temperature sputtered-SnO2 modified anode toward efficient TiO2-based planar perovskite solar cells. Science China Technological Sciences, 2021, 64, 1995-2002.	2.0	6
116	An in-situ defect passivation through a green anti-solvent approach for high-efficiency and stable perovskite solar cells. Science Bulletin, 2021, 66, 1419-1428.	4.3	29
117	<i>&gt;m</i> -Phenylenediammonium as a New Spacer for Dion–Jacobson Two-Dimensional Perovskites. Journal of the American Chemical Society, 2021, 143, 12063-12073.	6.6	71
118	pâ€Type Carbon Dots for Effective Surface Optimization for Nearâ€Recordâ€Efficiency CsPbl <sub>2</sub> Br Solar Cells. Small, 2021, 17, e2102272.	5.2	34
119	Secondary crystallization strategy for highly efficient inorganic CsPbI2Br perovskite solar cells with efficiency approaching 17%. Journal of Energy Chemistry, 2021, 63, 558-565.	7.1	22
120	A Special Additive Enables All Cations and Anions Passivation for Stable Perovskite Solar Cells with Efficiency over 23%. Nano-Micro Letters, 2021, 13, 169.	14.4	86
121	Pyrenesulfonic Acid Sodium Salt for Effective Bottomâ€Surface Passivation to Attain High Performance of Perovskite Solar Cells. Solar Rrl, 2021, 5, 2100416.	3.1	8
122	Defects in CsPbX <sub>3</sub> Perovskite: From Understanding to Effective Manipulation for Highâ€Performance Solar Cells. Small Methods, 2021, 5, e2100725.	4.6	37
123	Moltenâ€Saltâ€Assisted CsPbl <sub>3</sub> Perovskite Crystallization for Nearly 20%â€Efficiency Solar Cells. Advanced Materials, 2021, 33, e2103770.	11.1	81
124	Interfaces and Interfacial Layers in Inorganic Perovskite Solar Cells. Angewandte Chemie, 2021, 133, 26644-26657.	1.6	14
125	Rational Surfaceâ€Defect Control via Designed Passivation for Highâ€Efficiency Inorganic Perovskite Solar Cells. Angewandte Chemie - International Edition, 2021, 60, 23164-23170.	7.2	189
126	Interfaces and Interfacial Layers in Inorganic Perovskite Solar Cells. Angewandte Chemie - International Edition, 2021, 60, 26440-26453.	7.2	69

#	Article	IF	CITATIONS
127	lrO <sub><i>x</i></sub> @In <sub>2</sub> O <sub>3</sub> Heterojunction from Individually Crystallized Oxides for Weak‣ightâ€Promoted Electrocatalytic Water Oxidation. Angewandte Chemie, 2021, 133, 26994-27001.	1.6	4
128	Rational Surfaceâ€Defect Control via Designed Passivation for Highâ€Efficiency Inorganic Perovskite Solar Cells. Angewandte Chemie, 2021, 133, 23348-23354.	1.6	58
129	IrO <sub><i>x</i></sub> @In <sub>2</sub> O <sub>3</sub> Heterojunction from Individually Crystallized Oxides for Weakâ€Lightâ€Promoted Electrocatalytic Water Oxidation. Angewandte Chemie - International Edition, 2021, 60, 26790-26797.	7.2	23
130	Dual Passivation of Perovskite and SnO <sub>2</sub> for Highâ€Efficiency MAPbI <sub>3</sub> Perovskite Solar Cells. Advanced Science, 2021, 8, 2001466.	5.6	72
131	Design of surface termination for high-performance perovskite solar cells. Journal of Materials Chemistry A, 2021, 9, 23597-23606.	5.2	25
132	Inner Strain Regulation in Perovskite Single Crystals through Fine-Tuned Halide Composition. Crystal Growth and Design, 2021, 21, 1741-1750.	1.4	14
133	A review on the stability of inorganic metal halide perovskites: challenges and opportunities for stable solar cells. Energy and Environmental Science, 2021, 14, 2090-2113.	15.6	193
134	Grain and stoichiometry engineering for ultra-sensitive perovskite X-ray detectors. Journal of Materials Chemistry A, 2021, 9, 25603-25610.	5.2	18
135	Flexible Diodes/Transistors Based on Tunable p-n-Type Semiconductivity in Graphene/Mn-Co-Ni-O Nanocomposites. Research, 2021, 2021, 9802795.	2.8	2
136	Nâ€Type Surface Design for pâ€Type CZTSSe Thin Film to Attain High Efficiency. Advanced Materials, 2021, 33, e2104330.	11.1	49
137	Graphene–MCN pn-junction for ultrafast flexible ultraviolet detector. MRS Communications, 2021, 11, 862.	0.8	0
138	Effective surface passivation with 4-bromo-benzonitrile to enhance the performance of perovskite solar cells. Journal of Materials Chemistry C, 2021, 9, 17089-17098.	2.7	7
139	Verringerung schÃ <b>d</b> licher Defekte für leistungsstarke Metallhalogenidâ€Perowskitâ€Solarzellen. Angewandte Chemie, 2020, 132, 6740-6764.	1.6	16
140	Reducing Detrimental Defects for Highâ€Performance Metal Halide Perovskite Solar Cells. Angewandte Chemie - International Edition, 2020, 59, 6676-6698.	7.2	334
141	Fabrication of efficient CsPbBr3 perovskite solar cells by single-source thermal evaporation. Journal of Alloys and Compounds, 2020, 818, 152903.	2.8	58
142	Improve the oxide/perovskite heterojunction contact for low temperature high efficiency and stable all-inorganic CsPbI2Br perovskite solar cells. Nano Energy, 2020, 67, 104241.	8.2	97
143	27%â€Efficiency Fourâ€Terminal Perovskite/Silicon Tandem Solar Cells by Sandwiched Gold Nanomesh. Advanced Functional Materials, 2020, 30, 1908298.	7.8	91
144	Ambient blade coating of mixed cation, mixed halide perovskites without dripping: <i>in situ</i> in vestigation and highly efficient solar cells. Journal of Materials Chemistry A, 2020, 8, 1095-1104.	5.2	68

#	Article	IF	CITATIONS
145	Novel inorganic electron transport layers for planar perovskite solar cells: Progress and prospective. Nano Energy, 2020, 68, 104289.	8.2	83
146	Reply to â€~Comment on "Zero-thermal-quenching and photoluminescence tuning with the assistance of carriers from defect cluster trapsâ€â€™. Journal of Materials Chemistry C, 2020, 8, 1153-1156.	2.7	0
147	Chlorineâ€modified SnO <sub>2</sub> electron transport layer for highâ€efficiency perovskite solar cells. InformaÄnÃ-Materiály, 2020, 2, 401-408.	8.5	48
148	NaCl-assisted defect passivation in the bulk and surface of TiO2 enhancing efficiency and stability of planar perovskite solar cells. Journal of Power Sources, 2020, 448, 227586.	4.0	26
149	Improvement of Colloidal Characteristics in a Precursor Solution by a PbI2-(DMSO)2 Complex for Efficient Nonstoichiometrically Prepared CsPbI2.8Br0.2 Perovskite Solar Cells. ACS Applied Materials & Interfaces, 2020, 12, 48756-48764.	4.0	10
150	Highâ€Pressure Nitrogenâ€Extraction and Effective Passivation to Attain Highest Largeâ€Area Perovskite Solar Module Efficiency. Advanced Materials, 2020, 32, e2004979.	11.1	145
151	Beach-Chair-Shaped Energy Band Alignment for High-Performance β-CsPbI3 Solar Cells. Cell Reports Physical Science, 2020, 1, 100180.	2.8	28
152	Polymeric room-temperature molten salt as a multifunctional additive toward highly efficient and stable inverted planar perovskite solar cells. Energy and Environmental Science, 2020, 13, 5068-5079.	15.6	121
153	2D Perovskite Single Crystals with Suppressed Ion Migration for Highâ€Performance Planarâ€Type Photodetectors. Small, 2020, 16, e2003145.	5.2	56
154	Morphology Evolution of a Highâ€Efficiency PSC by Modulating the Vapor Process. Small, 2020, 16, e2003582.	5.2	15
155	The Possible Side Reaction in the Annealing Process of Perovskite Layers. ACS Applied Materials & Interfaces, 2020, 12, 35043-35048.	4.0	10
156	Surface Engineering to Reduce the Interfacial Resistance for Enhanced Photocatalytic Water Oxidation. ACS Catalysis, 2020, 10, 8742-8750.	5.5	26
157	Defect suppression in multinary chalcogenide photovoltaic materials derived from kesterite: progress and outlook. Journal of Materials Chemistry A, 2020, 8, 24920-24942.	5.2	36
158	A temperature gradient-induced directional growth of a perovskite film. Journal of Materials Chemistry A, 2020, 8, 17019-17024.	5.2	7
159	2D Cs <sub>2</sub> PbI <sub>2</sub> Cl <sub>2</sub> Nanosheets for Holistic Passivation of Inorganic CsPbI <sub>2</sub> Br Perovskite Solar Cells for Improved Efficiency and Stability. Advanced Energy Materials, 2020, 10, 2002882.	10.2	105
160	Ultrastable Perovskite–Zeolite Composite Enabled by Encapsulation and In Situ Passivation. Angewandte Chemie - International Edition, 2020, 59, 23100-23106.	7.2	75
161	Cd-Doped Triple-Cation Perovskite Thin Films with a 20 μs Carrier Lifetime. Journal of Physical Chemistry C, 2020, 124, 22011-22018.	1.5	10
162	Metalâ€Free Halide Perovskite Single Crystals with Very Long Charge Lifetimes for Efficient Xâ€ray Imaging. Advanced Materials, 2020, 32, e2003353.	11.1	68

#	Article	IF	CITATIONS
163	Printable CsPbI <sub>3</sub> Perovskite Solar Cells with PCE of 19% via an Additive Strategy. Advanced Materials, 2020, 32, e2001243.	11.1	157
164	Ultrastable Perovskite–Zeolite Composite Enabled by Encapsulation and Inâ€Situ Passivation. Angewandte Chemie, 2020, 132, 23300-23306.	1.6	7
165	Interface Modification of a Perovskite/Hole Transport Layer with Tetraphenyldibenzoperiflanthene for Highly Efficient and Stable Solar Cells. ACS Applied Materials & Interfaces, 2020, 12, 45073-45082.	4.0	12
166	Increasing gas sensitivity of Co3O4 octahedra by tuning Co-Co3O4 (111) surface structure and sensing mechanism of 3-coordinated Co atom as an active center. Journal of Materials Science: Materials in Electronics, 2020, 31, 8852-8864.	1.1	6
167	Centimeterâ€6ized Single Crystal of Twoâ€Dimensional Halide Perovskites Incorporating Straightâ€Chain Symmetric Diammonium Ion for Xâ€Ray Detection. Angewandte Chemie - International Edition, 2020, 59, 14896-14902.	7.2	124
168	2D–3D Cs <sub>2</sub> PbI <sub>2</sub> Cl <sub>2</sub> –CsPbI <sub>2.5</sub> Br <sub>0.5</sub> Mixed-Dimensional Films for All-Inorganic Perovskite Solar Cells with Enhanced Efficiency and Stability. Journal of Physical Chemistry Letters, 2020, 11, 4138-4146.	2.1	40
169	Improved Interface Contact for Highly Stable All-Inorganic CsPbI <sub>2</sub> Br Planar Perovskite Solar Cells. ACS Applied Energy Materials, 2020, 3, 5173-5181.	2.5	16
170	Nucleation-controlled growth of superior lead-free perovskite Cs3Bi2I9 single-crystals for high-performance X-ray detection. Nature Communications, 2020, 11, 2304.	5.8	286
171	Mn Doping of CsPbl <sub>3</sub> Film Towards High-Efficiency Solar Cell. ACS Applied Energy Materials, 2020, 3, 5190-5197.	2.5	56
172	Inch-Size 0D-Structured Lead-Free Perovskite Single Crystals for Highly Sensitive Stable X-Ray Imaging. Matter, 2020, 3, 180-196.	5.0	202
173	Perspective on the imaging device based on perovskite materials. Journal of Semiconductors, 2020, 41, 050401.	2.0	5
174	Solvent Engineering Using a Volatile Solid for Highly Efficient and Stable Perovskite Solar Cells. Advanced Science, 2020, 7, 1903250.	5.6	47
175	Fabrication of nanoporous Ni and NiO via a dealloying strategy for water oxidation catalysis. Journal of Energy Chemistry, 2020, 50, 125-134.	7.1	34
176	Large and Dense Organic–Inorganic Hybrid Perovskite CH <sub>3</sub> NH <sub>3</sub> PbI <sub>3</sub> Wafer Fabricated by One-Step Reactive Direct Wafer Production with High X-ray Sensitivity. ACS Applied Materials & Interfaces, 2020, 12, 16592-16600.	4.0	94
177	Photo-Redeposition Synthesis of Bimetal Pt–Cu Co-catalysts for TiO <sub>2</sub> Photocatalytic Solar-Fuel Production. ACS Sustainable Chemistry and Engineering, 2020, 8, 6055-6064.	3.2	39
178	Efficient perovskite solar cells <i>via</i> surface passivation by a multifunctional small organic ionic compound. Journal of Materials Chemistry A, 2020, 8, 8313-8322.	5.2	68
179	Unveiling the Effects of Hydrolysisâ€Derived DMAI/DMAPbI <i><sub>x</sub></i> Intermediate Compound on the Performance of CsPbI <sub>3</sub> Solar Cells. Advanced Science, 2020, 7, 1902868.	5.6	97
180	Direct Growth of Pyramidâ€Textured Perovskite Single Crystals: A New Strategy for Enhanced Optoelectronic Performance. Advanced Functional Materials, 2020, 30, 2002742.	7.8	20

#	Article	IF	CITATIONS
181	Lowâ€Temperature Crystallization of CsPbIBr <sub>2</sub> Perovskite for High Performance Solar Cells. Solar Rrl, 2020, 4, 2000254.	3.1	31
182	Large Leadâ€Free Perovskite Single Crystal for Highâ€Performance Coplanar Xâ€Ray Imaging Applications. Advanced Optical Materials, 2020, 8, 2000814.	3.6	67
183	Recent progress of twoâ€dimensional lead halide perovskite single crystals: Crystal growth, physical properties, and device applications. EcoMat, 2020, 2, e12036.	6.8	80
184	Deepâ€Ultraviolet Photoactivationâ€Assisted Contact Engineering Toward Highâ€Efficiency and Stable Allâ€Inorganic CsPbI <sub>2</sub> Br Perovskite Solar Cells. Solar Rrl, 2020, 4, 2000001.	3.1	29
185	Controlled nâ€Doping in Airâ€Stable CsPbI <sub>2</sub> Br Perovskite Solar Cells with a Record Efficiency of 16.79%. Advanced Functional Materials, 2020, 30, 1909972.	7.8	282
186	Anthradithiophene based hole-transport material for efficient and stable perovskite solar cells. Journal of Energy Chemistry, 2020, 48, 293-298.	7.1	16
187	Facile synthesis of "lucky clover―hole-transport material for efficient and stable large-area perovskite solar cells. Journal of Power Sources, 2020, 454, 227938.	4.0	11
188	Triphenylamine-based hole transporting materials with thiophene-derived bridges for perovskite solar cells. Synthetic Metals, 2020, 261, 116323.	2.1	10
189	Roomâ€Temperature Partial Conversion of αâ€FAPbI <sub>3</sub> Perovskite Phase via PbI <sub>2</sub> Solvation Enables Highâ€Performance Solar Cells. Advanced Functional Materials, 2020, 30, 1907442.	7.8	41
190	Consensus statement for stability assessment and reporting for perovskite photovoltaics based on ISOS procedures. Nature Energy, 2020, 5, 35-49.	19.8	797
191	Superior Textured Film and Process Tolerance Enabled by Intermediateâ€State Engineering for Highâ€Efficiency Perovskite Solar Cells. Advanced Science, 2020, 7, 1903009.	5.6	22
192	Enabling Unassisted Solar Water Splitting by Single-Junction Amorphous Silicon Photoelectrodes. ACS Applied Energy Materials, 2020, 3, 4629-4637.	2.5	11
193	Extrinsic Ion Distribution Induced Field Effect in CsPbIBr <sub>2</sub> Perovskite Solar Cells. Small, 2020, 16, e1907283.	5.2	44
194	Highâ€Efficiency Perovskite Solar Cells Enabled by Anatase TiO <sub>2</sub> Nanopyramid Arrays with an Oriented Electric Field. Angewandte Chemie - International Edition, 2020, 59, 11969-11976.	7.2	76
195	Precursor Engineering for Ambientâ€Compatible Antisolventâ€Free Fabrication of Highâ€Efficiency CsPbl <sub>2</sub> Br Perovskite Solar Cells. Advanced Energy Materials, 2020, 10, 2000691.	10.2	106
196	High‣fficiency Perovskite Solar Cells Enabled by Anatase TiO <sub>2</sub> Nanopyramid Arrays with an Oriented Electric Field. Angewandte Chemie, 2020, 132, 12067-12074.	1.6	15
197	Highly stable and efficient perovskite solar cells produced via high-boiling point solvents and additive engineering synergistically. Science China Chemistry, 2020, 63, 818-826.	4.2	11
198	Centimeterâ€Sized Single Crystal of Twoâ€Dimensional Halide Perovskites Incorporating Straightâ€Chain Symmetric Diammonium Ion for Xâ€Ray Detection. Angewandte Chemie, 2020, 132, 15006-15012.	1.6	11

#	Article	IF	CITATIONS
199	High detectivity photodetectors based on perovskite nanowires with suppressed surface defects. Photonics Research, 2020, 8, 1862.	3.4	23
200	CsPb(I Br1â^')3 solar cells. Science Bulletin, 2019, 64, 1532-1539.	4.3	114
201	Highly Efficient and Stable Planar Perovskite Solar Cells with Modulated Diffusion Passivation Toward High Power Conversion Efficiency and Ultrahigh Fill Factor. Solar Rrl, 2019, 3, 1900293.	3.1	87
202	Scalable Fabrication of Metal Halide Perovskite Solar Cells and Modules. ACS Energy Letters, 2019, 4, 2147-2167.	8.8	161
203	Pseudohalide induced tunable electronic and excitonic properties in two-dimensional single-layer perovskite for photovoltaics and photoelectronic applications. Journal of Energy Chemistry, 2019, 36, 106-113.	7.1	10
204	Metal Cations in Efficient Perovskite Solar Cells: Progress and Perspective. Advanced Materials, 2019, 31, e1902037.	11.1	71
205	Highly efficient and stable planar CsPbI2Br perovskite solar cell with a new sensitive-dopant-free hole transport layer obtained via an effective surface passivation. Solar Energy Materials and Solar Cells, 2019, 201, 110052.	3.0	45
206	Effective electron extraction from active layer for enhanced photodetection of photoconductive type detector with structure of Au/CH3NH3PbI3/Au. Organic Electronics, 2019, 74, 197-203.	1.4	6
207	Ligand-Size Related Dimensionality Control in Metal Halide Perovskites. ACS Energy Letters, 2019, 4, 1830-1838.	8.8	38
208	Abnormal absorption onset shift of CH3NH3PbI3 film by adding PbBr2 into its precursor and its effect on photovoltaic performance. Journal of Power Sources, 2019, 437, 226914.	4.0	8
209	Additive Engineering to Grow Micronâ€5ized Grains for Stable High Efficiency Perovskite Solar Cells. Advanced Science, 2019, 6, 1901241.	5.6	93
210	A High Mobility Conjugated Polymer Enables Air and Thermally Stable CsPbI <sub>2</sub> Br Perovskite Solar Cells with an Efficiency Exceeding 15%. Advanced Materials Technologies, 2019, 4, 1900311.	3.0	59
211	Cesium Lead Mixed-Halide Perovskites for Low-Energy Loss Solar Cells with Efficiency Beyond 17%. Chemistry of Materials, 2019, 31, 6231-6238.	3.2	76
212	Moisture-Induced Crystallinity Improvement for Efficient CsPbI <sub>3–<i>x</i></sub> Br <i><sub><i>x</i></sub></i> Perovskite Solar Cells with Excess Cesium Bromide. Journal of Physical Chemistry Letters, 2019, 10, 4587-4595.	2.1	20
213	Interfacial TiO2 atomic layer deposition triggers simultaneous crystallization control and band alignment for efficient CsPbIBr2 perovskite solar cell. Organic Electronics, 2019, 74, 103-109.	1.4	27
214	Simultaneous Cesium and Acetate Coalloying Improves Efficiency and Stability of FA <sub>0.85</sub> MA <sub>0.15</sub> PbI <sub>3</sub> Perovskite Solar Cell with an Efficiency of 21.95%. Solar Rrl, 2019, 3, 1900220.	3.1	74
215	Layer-Dependent Ultrahigh-Mobility Transport Properties in All-Inorganic Two-Dimensional Cs <sub>2</sub> PbI <sub>2</sub> Cl <sub>2</sub> and Cs <sub>2</sub> SnI <sub>2</sub> Cl <sub>2</sub> Perovskites. Journal of Physical Chemistry C, 2019, 123, 27978-27985.	1.5	45
216	Compositional Control in 2D Perovskites with Alternating Cations in the Interlayer Space for Photovoltaics with Efficiency over 18%. Advanced Materials, 2019, 31, e1903848.	11.1	171

#	Article	IF	CITATIONS
217	Fine Multiâ€Phase Alignments in 2D Perovskite Solar Cells with Efficiency over 17% via Slow Postâ€Annealing. Advanced Materials, 2019, 31, e1903889.	11.1	178
218	Ruddlesden–Popper 2D Component to Stabilize γ sPbl <sub>3</sub> Perovskite Phase for Stable and Efficient Photovoltaics. Advanced Energy Materials, 2019, 9, 1902529.	10.2	111
219	Europium and Acetate Coâ€doping Strategy for Developing Stable and Efficient CsPbI <sub>2</sub> Br Perovskite Solar Cells. Small, 2019, 15, e1904387.	5.2	95
220	Photoassisted Hydrothermal Synthesis of IrOx–TiO <sub>2</sub> for Enhanced Water Oxidation. ACS Sustainable Chemistry and Engineering, 2019, 7, 17941-17949.	3.2	18
221	A Novel Anion Doping for Stable CsPbI <sub>2</sub> Br Perovskite Solar Cells with an Efficiency of 15.56% and an Open Circuit Voltage of 1.30 V. Advanced Energy Materials, 2019, 9, 1902279.	10.2	166
222	Direct–Indirect Transition of Pressurized Two-Dimensional Halide Perovskite: Role of Benzene Ring Stack Ordering. Journal of Physical Chemistry Letters, 2019, 10, 5687-5693.	2.1	20
223	Scalable Ambient Fabrication of High-Performance CsPbI2Br Solar Cells. Joule, 2019, 3, 2485-2502.	11.7	124
224	Interfacial Engineering at the 2D/3D Heterojunction for High-Performance Perovskite Solar Cells. Nano Letters, 2019, 19, 7181-7190.	4.5	163
225	Photoelectrochemical CO <sub>2</sub> reduction to adjustable syngas on grain-boundary-mediated a-Si/TiO <sub>2</sub> /Au photocathodes with low onset potentials. Energy and Environmental Science, 2019, 12, 923-928.	15.6	114
226	A straightforward chemical approach for excellent In <sub>2</sub> S <sub>3</sub> electron transport layer for high-efficiency perovskite solar cells. RSC Advances, 2019, 9, 884-890.	1.7	21
227	NbF <sub>5</sub> : A Novel αâ€Phase Stabilizer for FAâ€Based Perovskite Solar Cells with High Efficiency. Advanced Functional Materials, 2019, 29, 1807850.	7.8	150
228	Perovskite—a Perfect Top Cell for Tandem Devices to Break the S–Q Limit. Advanced Science, 2019, 6, 1801704.	5.6	80
229	Impact of the Solvation State of Lead Iodide on Its Twoâ€Step Conversion to MAPbI <sub>3</sub> : An In Situ Investigation. Advanced Functional Materials, 2019, 29, 1807544.	7.8	45
230	Chlorine doping for black Î <sup>3</sup> -CsPbI3 solar cells with stabilized efficiency beyond 16%. Nano Energy, 2019, 58, 175-182.	8.2	170
231	Two-dimensional (PEA) <sub>2</sub> PbBr <sub>4</sub> perovskite single crystals for a high performance UV-detector. Journal of Materials Chemistry C, 2019, 7, 1584-1591.	2.7	138
232	First-Principles Study of Enhanced Out-of-Plane Transport Properties and Stability in Dion–Jacobson Two-Dimensional Perovskite Semiconductors for High-Performance Solar Cell Applications. Journal of Physical Chemistry Letters, 2019, 10, 3670-3675.	2.1	42
233	Chemical Bath Deposition of Coâ€Doped TiO <sub>2</sub> Electron Transport Layer for Hysteresisâ€Suppressed Highâ€Efficiency Planar Perovskite Solar Cells. Solar Rrl, 2019, 3, 1900176.	3.1	36
234	Single-crystalline lead halide perovskite wafers for high performance photodetectors. Journal of Materials Chemistry C, 2019, 7, 8357-8363.	2.7	33

#	Article	IF	CITATIONS
235	Comprehensive investigation of sputtered and spin-coated zinc oxide electron transport layers for highly efficient and stable planar perovskite solar cells. Journal of Power Sources, 2019, 427, 223-230.	4.0	24
236	Single atom tungsten doped ultrathin α-Ni(OH)2 for enhanced electrocatalytic water oxidation. Nature Communications, 2019, 10, 2149.	5.8	363
237	Surface-Tension-Controlled Crystallization for High-Quality 2D Perovskite Single Crystals for Ultrahigh Photodetection. Matter, 2019, 1, 465-480.	5.0	202
238	Increasing Quantum Efficiency of Polymer Solar Cells with Efficient Exciton Splitting and Long Carrier Lifetime by Molecular Doping at Heterojunctions. ACS Energy Letters, 2019, 4, 1356-1363.	8.8	45
239	Hydrogenated nanotubes/nanowires assembled from TiO <sub>2</sub> nanoflakes with exposed {111} facets: excellent photo-catalytic CO <sub>2</sub> reduction activity and charge separation mechanism between (111) and (1̄1̄1̄) polar surfaces. Journal of Materials Chemistry A, 2019, 7, 14761-14775.	5.2	31
240	Goldschmidt-rule-deviated perovskite CsPbIBr2by barium substitution for efficient solar cells. Nano Energy, 2019, 61, 165-172.	8.2	93
241	Origin of enhanced stability in thiocyanate substituted α-FAPbI3 analogues. Science China Chemistry, 2019, 62, 866-874.	4.2	12
242	Stable Efficiency Exceeding 20.6% for Inverted Perovskite Solar Cells through Polymer-Optimized PCBM Electron-Transport Layers. Nano Letters, 2019, 19, 3313-3320.	4.5	181
243	Double‣ite Ni–W Nanosheet for Best Alkaline HER Performance at High Current Density >500 mA cm <sup>â^²2</sup> . Advanced Materials Interfaces, 2019, 6, 1900308.	1.9	24
244	Anorganische CsPbX <sub>3</sub> â€Perowskitâ€Solarzellen: Fortschritte und Perspektiven. Angewandte Chemie, 2019, 131, 15742-15765.	1.6	20
245	Allâ€Inorganic CsPbX <sub>3</sub> Perovskite Solar Cells: Progress and Prospects. Angewandte Chemie - International Edition, 2019, 58, 15596-15618.	7.2	425
246	Effect of TC(002) on the Output Current of a ZnO Thin-Film Nanogenerator and a New Piezoelectricity Mechanism at the Atomic Level. ACS Applied Materials & Interfaces, 2019, 11, 12656-12665.	4.0	27
247	Novel Surface Passivation for Stable FA <sub>0.85</sub> MA <sub>0.15</sub> PbI <sub>3</sub> Perovskite Solar Cells with 21.6% Efficiency. Solar Rrl, 2019, 3, 1900072.	3.1	64
248	Thermally stable methylammonium-free inverted perovskite solar cells with Zn2+ doped CuGaO2 as efficient mesoporous hole-transporting layer. Nano Energy, 2019, 61, 148-157.	8.2	90
249	Interfaceâ€Modificationâ€Induced Gradient Energy Band for Highly Efficient CsPblBr <sub>2</sub> Perovskite Solar Cells. Advanced Energy Materials, 2019, 9, 1803785.	10.2	191
250	Interface engineering of low temperature processed all-inorganic CsPbI2Br perovskite solar cells toward PCE exceeding 14%. Nano Energy, 2019, 60, 583-590.	8.2	135
251	Lowâ€Temperature Solutionâ€Processed ZnO Electron Transport Layer for Highly Efficient and Stable Planar Perovskite Solar Cells with Efficiency Over 20%. Solar Rrl, 2019, 3, 1900096.	3.1	66
252	Oxidation, reduction, and inert gases plasma-modified defects in TiO2 as electron transport layer for planar perovskite solar cells. Journal of CO2 Utilization, 2019, 32, 46-52.	3.3	8

#	Article	IF	CITATIONS
253	Improving sensing performance of the ZnO foam structure with exposed {001} facets by hydrogenation and sensing mechanism at molecule level. Applied Surface Science, 2019, 479, 646-654.	3.1	22
254	Waterâ€Soluble Triazolium Ionicâ€Liquidâ€Induced Surface Selfâ€Assembly to Enhance the Stability and Efficiency of Perovskite Solar Cells. Advanced Functional Materials, 2019, 29, 1900417.	7.8	145
255	Nitrogen-doped graphene quantum dots for 80% photoluminescence quantum yield for inorganic γ-CsPbI <sub>3</sub> perovskite solar cells with efficiency beyond 16%. Journal of Materials Chemistry A, 2019, 7, 5740-5747.	5.2	113
256	Optical Management with Nanoparticles for a Light Conversion Efficiency Enhancement in Inorganic γ-CsPbl <sub>3</sub> Solar Cells. Nano Letters, 2019, 19, 1796-1804.	4.5	58
257	Influence of Film Quality on Power Conversion Efficiency in Perovskite Solar Cells. Coatings, 2019, 9, 622.	1.2	8
258	Pseudohalide (SCN <sup>â^'</sup> )-doped CsPbI <sub>3</sub> for high-performance solar cells. Journal of Materials Chemistry C, 2019, 7, 13736-13742.	2.7	53
259	The humidity-insensitive fabrication of efficient CsPbI <sub>3</sub> solar cells in ambient air. Journal of Materials Chemistry A, 2019, 7, 26776-26784.	5.2	54
260	Low-temperature-gradient crystallization for multi-inch high-quality perovskite single crystals for record performance photodetectors. Materials Today, 2019, 22, 67-75.	8.3	204
261	Fabrication of a High-Quality Cu <sub>2</sub> ZnSn(S,Se) <sub>4</sub> Absorber Layer via an Aqueous Solution Process and Application in Solar Cells. ACS Applied Materials & Interfaces, 2019, 11, 634-639.	4.0	9
262	Two dimensional metal halide perovskites: Promising candidates for light-emitting diodes. Journal of Energy Chemistry, 2019, 37, 97-110.	7.1	52
263	Record‣owâ€Threshold Lasers Based on Atomically Smooth Triangular Nanoplatelet Perovskite. Advanced Functional Materials, 2019, 29, 1805553.	7.8	52
264	PbTiO <sub>3</sub> as Electronâ€Selective Layer for Highâ€Efficiency Perovskite Solar Cells: Enhanced Electron Extraction via Tunable Ferroelectric Polarization. Advanced Functional Materials, 2019, 29, 1806427.	7.8	23
265	Roomâ€Temperature Surface Sulfurization for Highâ€Performance Kesterite CZTSe Solar Cells. Solar Rrl, 2019, 3, 1800236.	3.1	21
266	Nanodevices: Record-Low-Threshold Lasers Based on Atomically Smooth Triangular Nanoplatelet Perovskite (Adv. Funct. Mater. 2/2019). Advanced Functional Materials, 2019, 29, 1970012.	7.8	1
267	Dynamical Transformation of Two-Dimensional Perovskites with Alternating Cations in the Interlayer Space for High-Performance Photovoltaics. Journal of the American Chemical Society, 2019, 141, 2684-2694.	6.6	189
268	Flexible Perowskit‧olarzellen: Herstellung und Anwendungen. Angewandte Chemie, 2019, 131, 4512-4530.	1.6	27
269	Recent Advances in Flexible Perovskite Solar Cells: Fabrication and Applications. Angewandte Chemie - International Edition, 2019, 58, 4466-4483.	7.2	290
270	Anti-solvent engineering for efficient semitransparent CH3NH3PbBr3 perovskite solar cells for greenhouse applications. Journal of Energy Chemistry, 2019, 34, 12-19.	7.1	50

#	Article	IF	CITATIONS
271	P-type sub-tungsten-oxide based urchin-like nanostructure for superior room temperature alcohol sensor. Applied Surface Science, 2018, 441, 277-284.	3.1	20
272	Interface engineering of CsPbBr3/TiO2 heterostructure with enhanced optoelectronic properties for all-inorganic perovskite solar cells. Applied Physics Letters, 2018, 112, .	1.5	60
273	Single-crystalline perovskite wafers with a Cr blocking layer for broad and stable light detection in a harsh environment. RSC Advances, 2018, 8, 14848-14853.	1.7	9
274	g <sub>3</sub> N <sub>4</sub> Loading Black Phosphorus Quantum Dot for Efficient and Stable Photocatalytic H <sub>2</sub> Generation under Visible Light. Advanced Functional Materials, 2018, 28, 1800668.	7.8	257
275	Phase Transition Control for High Performance Ruddlesden–Popper Perovskite Solar Cells. Advanced Materials, 2018, 30, e1707166.	11.1	244
276	Controlled defects and enhanced electronic extraction in fluorine-incorporated zinc oxide for high-performance planar perovskite solar cells. Solar Energy Materials and Solar Cells, 2018, 182, 263-271.	3.0	41
277	Ge quantum-dot enhanced c-Si solar cell for improved light trapping efficiency. Solar Energy, 2018, 167, 102-107.	2.9	10
278	Chelate-Pb Intermediate Engineering for High-Efficiency Perovskite Solar Cells. ACS Applied Materials & Interfaces, 2018, 10, 14744-14750.	4.0	15
279	Low-temperature and facile solution-processed two-dimensional TiS <sub>2</sub> as an effective electron transport layer for UV-stable planar perovskite solar cells. Journal of Materials Chemistry A, 2018, 6, 9132-9138.	5.2	78
280	Bifunctional Hydroxylamine Hydrochloride Incorporated Perovskite Films for Efficient and Stable Planar Perovskite Solar Cells. ACS Applied Energy Materials, 2018, 1, 900-909.	2.5	81
281	Flexible perovskite solar cells based on green, continuous roll-to-roll printing technology. Journal of Energy Chemistry, 2018, 27, 971-989.	7.1	55
282	All-Ambient Processed Binary CsPbBr <sub>3</sub> –CsPb <sub>2</sub> Br <sub>5</sub> Perovskites with Synergistic Enhancement for High-Efficiency Cs–Pb–Br-Based Solar Cells. ACS Applied Materials & Interfaces, 2018, 10, 7145-7154.	4.0	171
283	Stoichiometry control of sputtered zinc oxide films by adjusting Ar/O2 gas ratios as electron transport layers for efficient planar perovskite solar cells. Solar Energy Materials and Solar Cells, 2018, 178, 200-207.	3.0	26
284	3D–2D–0D Interface Profiling for Record Efficiency Allâ€Inorganic CsPbBrl <sub>2</sub> Perovskite Solar Cells with Superior Stability. Advanced Energy Materials, 2018, 8, 1703246.	10.2	301
285	Shape―and Trap ontrolled Nanocrystals for Giantâ€Performance Improvement of Allâ€Inorganic Perovskite Photodetectors. Particle and Particle Systems Characterization, 2018, 35, 1700363.	1.2	24
286	Alkali Metal Doping for Improved CH <sub>3</sub> NH <sub>3</sub> PbI <sub>3</sub> Perovskite Solar Cells. Advanced Science, 2018, 5, 1700131.	5.6	227
287	Electronic and magnetic behaviors of B, N, and 3d transition metal substitutions in germanium carbide monolayer. Journal of Magnetism and Magnetic Materials, 2018, 451, 799-807.	1.0	15
288	µâ€Graphene Crosslinked CsPbI <sub>3</sub> Quantum Dots for High Efficiency Solar Cells with Much Improved Stability. Advanced Energy Materials, 2018, 8, 1800007.	10.2	198

#	Article	IF	CITATIONS
289	Realizing efficient red thermally activated delayed fluorescence organic light-emitting diodes using phenoxazine/phenothiazine-phenanthrene hybrids. Organic Electronics, 2018, 59, 32-38.	1.4	35
290	Highâ€Performance Planar Perovskite Solar Cells Using Low Temperature, Solution–Combustionâ€Based Nickel Oxide Hole Transporting Layer with Efficiency Exceeding 20%. Advanced Energy Materials, 2018, 8, 1703432.	10.2	279
291	Hydrogenated TiO2 nanosheet based flowerlike architectures: Enhanced sensing performances and sensing mechanism. Journal of Alloys and Compounds, 2018, 749, 543-555.	2.8	14
292	Interstitial Mn <sup>2+</sup> -Driven High-Aspect-Ratio Grain Growth for Low-Trap-Density Microcrystalline Films for Record Efficiency CsPbI <sub>2</sub> Br Solar Cells. ACS Energy Letters, 2018, 3, 970-978.	8.8	356
293	Stable Highâ€Performance Perovskite Solar Cells via Grain Boundary Passivation. Advanced Materials, 2018, 30, e1706576.	11.1	665
294	Enhanced luminescence and tunable color of Sr8CaSc(PO4)7:Eu2+, Ce3+, Mn2+ phosphor by energy transfer between Ce3+-Eu2+-Mn2+. Journal of Alloys and Compounds, 2018, 731, 796-804.	2.8	40
295	Path towards high-efficient kesterite solar cells. Journal of Energy Chemistry, 2018, 27, 1040-1053.	7.1	68
296	Polymer Doping for Highâ€Efficiency Perovskite Solar Cells with Improved Moisture Stability. Advanced Energy Materials, 2018, 8, 1701757.	10.2	293
297	Graphdiyne Quantum Dots for Much Improved Stability and Efficiency of Perovskite Solar Cells. Advanced Materials Interfaces, 2018, 5, 1701117.	1.9	76
298	Graphdiyne-WS2 2D-Nanohybrid electrocatalysts for high-performance hydrogen evolution reaction. Carbon, 2018, 129, 228-235.	5.4	124
299	WO 3 -SnO 2 nanosheet composites: Hydrothermal synthesis and gas sensing mechanism. Journal of Alloys and Compounds, 2018, 736, 322-331.	2.8	82
300	High-quality perovskite MAPbI3 single crystals for broad-spectrum and rapid response integrate photodetector. Journal of Energy Chemistry, 2018, 27, 722-727.	7.1	76
301	Recent Progress in Singleâ€Crystalline Perovskite Research Including Crystal Preparation, Property Evaluation, and Applications. Advanced Science, 2018, 5, 1700471.	5.6	223
302	Vapor-fumigation for record efficiency two-dimensional perovskite solar cells with superior stability. Energy and Environmental Science, 2018, 11, 3349-3357.	15.6	87
303	High performance ambient-air-stable FAPbI <sub>3</sub> perovskite solar cells with molecule-passivated Ruddlesden–Popper/3D heterostructured film. Energy and Environmental Science, 2018, 11, 3358-3366.	15.6	196
304	Sputtered ZnO Films as Electron Transport Layers for Efficient Planar Perovskite Solar Cells. , 2018, , .		2
305	Magnetic Field Driven Larger Grain Growth for Perovskite Film with Enhanced Photovoltaic Performance. , 2018, , .		1
306	Multi-inch single-crystalline perovskite membrane for high-detectivity flexible photosensors. Nature Communications, 2018, 9, 5302.	5.8	212

#	Article	IF	CITATIONS
307	Air-stable phosphorus-doped molybdenum nitride for enhanced electrocatalytic hydrogen evolution. Communications Chemistry, 2018, 1, .	2.0	36
308	Green Atmospheric Aqueous Solution Deposition for High Performance Cu 2 ZnSn(S,Se) 4 Thin Film Solar Cells. Solar Rrl, 2018, 2, 1800233.	3.1	16
309	Gas-solid reaction based over one-micrometer thick stable perovskite films for efficient solar cells and modules. Nature Communications, 2018, 9, 3880.	5.8	109
310	Design of an Inorganic Mesoporous Holeâ€Transporting Layer for Highly Efficient and Stable Inverted Perovskite Solar Cells. Advanced Materials, 2018, 30, e1805660.	11.1	179
311	Synergy of Hydrophobic Surface Capping and Lattice Contraction for Stable and Highâ€Efficiency Inorganic CsPbl <sub>2</sub> Br Perovskite Solar Cells. Solar Rrl, 2018, 2, 1800216.	3.1	68
312	Iodineâ€Optimized Interface for Inorganic CsPbI <sub>2</sub> Br Perovskite Solar Cell to Attain High Stabilized Efficiency Exceeding 14%. Advanced Science, 2018, 5, 1801123.	5.6	90
313	In Situ Grain Boundary Modification via Two-Dimensional Nanoplates to Remarkably Improve Stability and Efficiency of Perovskite Solar Cells. ACS Applied Materials & Interfaces, 2018, 10, 39802-39808.	4.0	24
314	All-inorganic cesium lead iodide perovskite solar cells with stabilized efficiency beyond 15%. Nature Communications, 2018, 9, 4544.	5.8	379
315	Quasiâ€Amorphous Metallic Nickel Nanopowder as an Efficient and Durable Electrocatalyst for Alkaline Hydrogen Evolution. Advanced Science, 2018, 5, 1801216.	5.6	37
316	Low Temperature Fabrication for High Performance Flexible CsPbI <sub>2</sub> Br Perovskite Solar Cells. Advanced Science, 2018, 5, 1801117.	5.6	96
317	Progress toward Stable Lead Halide Perovskite Solar Cells. Joule, 2018, 2, 1961-1990.	11.7	181
318	A Twoâ€ <b>£</b> tage Annealing Strategy for Crystallization Control of CH <sub>3</sub> NH <sub>3</sub> PbI <sub>3</sub> Films toward Highly Reproducible Perovskite Solar Cells. Small, 2018, 14, e1800181.	5.2	23
319	CsPbCl <sub>3</sub> â€Driven Lowâ€Trapâ€Density Perovskite Grain Growth for >20% Solar Cell Efficiency. Advanced Science, 2018, 5, 1800474.	5.6	65
320	Improving the Quality of CH <sub>3</sub> NH <sub>3</sub> PbI <sub>3</sub> Films via Chlorobenzene Vapor Annealing. Physica Status Solidi (A) Applications and Materials Science, 2018, 215, 1700959.	0.8	14
321	A 1300 mm <sup>2</sup> Ultrahighâ€Performance Digital Imaging Assembly using Highâ€Quality Perovskite Single Crystals. Advanced Materials, 2018, 30, e1707314.	11.1	246
322	Lowâ€Temperatureâ€Processed CdS as the Electron Selective Layer in an Organometal Halide Perovskite Photovoltaic Device. Particle and Particle Systems Characterization, 2018, 35, 1800137.	1.2	4
323	Enhanced Visible-Light Photocatalytic H <sub>2</sub> Evolution in Cu <sub>2</sub> O/Cu <sub>2</sub> Se Multilayer Heterostructure Nanowires Having {111} Facets and Physical Mechanism. Inorganic Chemistry, 2018, 57, 8019-8027.	1.9	23
324	Exposed the mechanism of lead chloride dopant for high efficiency planar-structure perovskite solar cells. Organic Electronics, 2018, 62, 499-504.	1.4	6

#	Article	IF	CITATIONS
325	Precursor Engineering for Allâ€Inorganic CsPbI <sub>2</sub> Br Perovskite Solar Cells with 14.78% Efficiency. Advanced Functional Materials, 2018, 28, 1803269.	7.8	264
326	Efficient planar CsPbBr3 perovskite solar cells by dual-source vacuum evaporation. Solar Energy Materials and Solar Cells, 2018, 187, 1-8.	3.0	139
327	Synergistic enhancement of Cs and Br doping in formamidinium lead halide perovskites for high performance optoelectronics. CrystEngComm, 2018, 20, 5510-5518.	1.3	6
328	The sensing reaction on the Ni-NiO (111) surface at atomic and molecule level and migration of electron. Sensors and Actuators B: Chemical, 2018, 273, 794-803.	4.0	19
329	"Heat Wave―of Metal Halide Perovskite Solar Cells Continues in Phoenix. ACS Energy Letters, 2018, 3, 1898-1903.	8.8	5
330	Record Efficiency Stable Flexible Perovskite Solar Cell Using Effective Additive Assistant Strategy. Advanced Materials, 2018, 30, e1801418.	11.1	377
331	Fe <sub>2</sub> O <sub>3</sub> /C–C <sub>3</sub> N <sub>4</sub> -Based Tight Heterojunction for Boosting Visible-Light-Driven Photocatalytic Water Oxidation. ACS Sustainable Chemistry and Engineering, 2018, 6, 10436-10444.	3.2	61
332	Highly efficient perovskite solar cells based on a dopant-free conjugated DPP polymer hole transport layer: influence of solvent vapor annealing. Sustainable Energy and Fuels, 2018, 2, 2154-2159.	2.5	24
333	Highly Efficient Ruddlesden–Popper Halide Perovskite PA <sub>2</sub> MA <sub>4</sub> Pb <sub>5</sub> 16 Solar Cells. ACS Energy Letters, 2018, 3, 1975-1982.	8.8	135
334	Phase Transition Control for High-Performance Blade-Coated Perovskite Solar Cells. Joule, 2018, 2, 1313-1330.	11.7	180
335	Graded Bandgap CsPbl2+Br1â^' Perovskite Solar Cells with a Stabilized Efficiency of 14.4%. Joule, 2018, 2, 1500-1510.	11.7	307
336	Giant Phonon Tuning Effect via Pressure-Manipulated Polar Rotation in Perovskite MAPbl <sub>3</sub> . Journal of Physical Chemistry Letters, 2018, 9, 3029-3034.	2.1	14
337	High efficiency planar-type perovskite solar cells with negligible hysteresis using EDTA-complexed SnO2. Nature Communications, 2018, 9, 3239.	5.8	1,017
338	Temperature-assisted crystallization for inorganic CsPbI2Br perovskite solar cells to attain high stabilized efficiency 14.81%. Nano Energy, 2018, 52, 408-415.	8.2	186
339	Zero-thermal-quenching and photoluminescence tuning with the assistance of carriers from defect cluster traps. Journal of Materials Chemistry C, 2018, 6, 10687-10692.	2.7	37
340	Nitrogen-promoted molybdenum dioxide nanosheets for electrochemical hydrogen generation. Journal of Materials Chemistry A, 2018, 6, 12532-12540.	5.2	34
341	Black Phosphorusâ€Based Compound with Few Layers for Photocatalytic Water Oxidation. ChemCatChem, 2018, 10, 3424-3428.	1.8	14
342	In Situ Synthesis of Fewâ€Layered g <sub>3</sub> N <sub>4</sub> with Vertically Aligned MoS <sub>2</sub> Loading for Boosting Solarâ€toâ€Hydrogen Generation. Small, 2018, 14, 1703003.	5.2	90

#	Article	IF	CITATIONS
343	Thickness Influence on Optical and Electrical Properties of PbI2 Films Prepared by Pulsed Laser Deposition. Science of Advanced Materials, 2018, 10, 701-706.	0.1	7
344	Enhancing the Sensing Properties of TiO <sub>2</sub> Nanosheets with Exposed {001} Facets by a Hydrogenation and Sensing Mechanism. Inorganic Chemistry, 2017, 56, 1504-1510.	1.9	50
345	Synthesis of a nano-sized hybrid C <sub>3</sub> N <sub>4</sub> /TiO <sub>2</sub> sample for enhanced and steady solar energy absorption and utilization. Sustainable Energy and Fuels, 2017, 1, 95-102.	2.5	22
346	Investigation of the mechanism responsible for the photoluminescence enhancement with Li + co-doping in highly thermally stable white-emitting Sr 8 ZnSc(PO 4 ) 7 :Dy 3+ phosphor. Journal of Luminescence, 2017, 187, 160-168.	1.5	10
347	Monolayer-by-monolayer growth of platinum films on complex carbon fiber paper structure. Applied Surface Science, 2017, 407, 386-390.	3.1	10
348	Superior Cu 2 S/brass-mesh electrode in CdS quantum dot sensitized solar cells for dual-side illumination. Materials Letters, 2017, 195, 100-103.	1.3	9
349	Ge quantum dot enhanced hydrogenated amorphous silicon germanium solar cells on flexible stainless steel substrate. Solar Energy, 2017, 144, 635-642.	2.9	6
350	The photovoltaic effect in a [001] orientated ZnO thin film and its physical mechanism. RSC Advances, 2017, 7, 9596-9604.	1.7	10
351	Stable ultra-fast broad-bandwidth photodetectors based on α-CsPbI <sub>3</sub> perovskite and NaYF <sub>4</sub> :Yb,Er quantum dots. Nanoscale, 2017, 9, 6278-6285.	2.8	93
352	Epitaxial growth of large-area and highly crystalline anisotropic ReSe2 atomic layer. Nano Research, 2017, 10, 2732-2742.	5.8	69
353	Organic–Inorganic Hybrid Perovskite with Controlled Dopant Modification and Application in Photovoltaic Device. Small, 2017, 13, 1604153.	5.2	59
354	Air and thermally stable perovskite solar cells with CVD-graphene as the blocking layer. Nanoscale, 2017, 9, 8274-8280.	2.8	58
355	P Doped MoO <sub>3â^'</sub> <i><sub>x</sub></i> Nanosheets as Efficient and Stable Electrocatalysts for Hydrogen Evolution. Small, 2017, 13, 1700441.	5.2	88
356	Solution Coating of Superior Largeâ€Area Flexible Perovskite Thin Films with Controlled Crystal Packing. Advanced Optical Materials, 2017, 5, 1700102.	3.6	34
357	Controllable synthesis of Ag-WO3 core-shell nanospheres for light-enhanced gas sensors. Sensors and Actuators B: Chemical, 2017, 251, 583-589.	4.0	35
358	Effect of argon flow on promoting boron doping for <i>in-situ</i> grown silicon nitride thin films containing silicon quantum dots. Nanotechnology, 2017, 28, 285202.	1.3	1
359	Highly thermally stable and emission color tunable borate glass for whiteâ€lightâ€emitting diodes with zero organic resin. Journal of the American Ceramic Society, 2017, 100, 4011-4020.	1.9	15
360	Enhanced sensing performance and sensing mechanism of hydrogenated NiO particles. Sensors and Actuators B: Chemical, 2017, 250, 208-214.	4.0	19

#	Article	IF	CITATIONS
361	ITIC surface modification to achieve synergistic electron transport layer enhancement for planar-type perovskite solar cells with efficiency exceeding 20%. Journal of Materials Chemistry A, 2017, 5, 9514-9522.	5.2	103
362	Room-Temperature Processed Nb <sub>2</sub> O <sub>5</sub> as the Electron-Transporting Layer for Efficient Planar Perovskite Solar Cells. ACS Applied Materials & Interfaces, 2017, 9, 23181-23188.	4.0	120
363	Stable High-Performance Flexible Photodetector Based on Upconversion Nanoparticles/Perovskite Microarrays Composite. ACS Applied Materials & Interfaces, 2017, 9, 19176-19183.	4.0	70
364	Magnetic Field-Assisted Perovskite Film Preparation for Enhanced Performance of Solar Cells. ACS Applied Materials & Interfaces, 2017, 9, 21756-21762.	4.0	27
365	Graphene-oxide doped PEDOT:PSS as a superior hole transport material for high-efficiency perovskite solar cell. Organic Electronics, 2017, 48, 165-171.	1.4	87
366	Energy-Down-Shift CsPbCl <sub>3</sub> :Mn Quantum Dots for Boosting the Efficiency and Stability of Perovskite Solar Cells. ACS Energy Letters, 2017, 2, 1479-1486.	8.8	221
367	Fe( <scp>iii</scp> ) doped NiS <sub>2</sub> nanosheet: a highly efficient and low-cost hydrogen evolution catalyst. Journal of Materials Chemistry A, 2017, 5, 10173-10181.	5.2	137
368	E-beam evaporated Nb2O5 as an effective electron transport layer for large flexible perovskite solar cells. Nano Energy, 2017, 36, 1-8.	8.2	215
369	Improvement of crystallinity for poly-Si thin film by negative substrate bias at low temperature. Thin Solid Films, 2017, 629, 90-96.	0.8	4
370	Enhancing Efficiency and Stability of Perovskite Solar Cells through Nb-Doping of TiO <sub>2</sub> at Low Temperature. ACS Applied Materials & Interfaces, 2017, 9, 10752-10758.	4.0	181
371	Solution-Processed Nb:SnO <sub>2</sub> Electron Transport Layer for Efficient Planar Perovskite Solar Cells. ACS Applied Materials & Interfaces, 2017, 9, 2421-2429.	4.0	315
372	Recent Advances in Photoelectrochemical Applications of Silicon Materials for Solarâ€to hemicals Conversion. ChemSusChem, 2017, 10, 4324-4341.	3.6	77
373	Synthesis of Largeâ€Size 1T′ ReS <sub>2</sub> <i><sub>x</sub></i> Se <sub>2(1â^'</sub> <i><sub>x</sub></i> <sub>)</sub> Alloy Monolayer with Tunable Bandgap and Carrier Type. Advanced Materials, 2017, 29, 1705015.	11.1	107
374	Cellular Architectureâ€Based Allâ€Polymer Flexible Thinâ€Film Photodetectors with High Performance and Stability in Harsh Environment. Advanced Materials Technologies, 2017, 2, 1700185.	3.0	7
375	CO <sub>2</sub> Plasma-Treated TiO <sub>2</sub> Film as an Effective Electron Transport Layer for High-Performance Planar Perovskite Solar Cells. ACS Applied Materials & Interfaces, 2017, 9, 33989-33996.	4.0	35
376	Earth-abundant elements doping for robust and stable solar-driven water splitting by FeOOH. Journal of Materials Chemistry A, 2017, 5, 21478-21485.	5.2	54
377	120 mm single-crystalline perovskite and wafers: towards viable applications. Science China Chemistry, 2017, 60, 1367-1376.	4.2	107
378	High-performance transparent ultraviolet photodetectors based on inorganic perovskite CsPbCl <sub>3</sub> nanocrystals. RSC Advances, 2017, 7, 36722-36727.	1.7	90

#	Article	IF	CITATIONS
379	Superior stability for perovskite solar cells with 20% efficiency using vacuum co-evaporation. Nanoscale, 2017, 9, 12316-12323.	2.8	169
380	Local temperature reduction induced crystallization of MASnI <sub>3</sub> and achieving a direct wafer production. RSC Advances, 2017, 7, 38155-38159.	1.7	17
381	Stable high efficiency two-dimensional perovskite solar cells via cesium doping. Energy and Environmental Science, 2017, 10, 2095-2102.	15.6	588
382	High-Performance, Self-Powered Photodetectors Based on Perovskite and Graphene. ACS Applied Materials & Interfaces, 2017, 9, 42779-42787.	4.0	91
383	Zn-doping for reduced hysteresis and improved performance of methylammonium lead iodide perovskite hybrid solar cells. Materials Today Energy, 2017, 5, 205-213.	2.5	75
384	Polar rotor scattering as atomic-level origin of low mobility and thermal conductivity of perovskite CH3NH3PbI3. Nature Communications, 2017, 8, 16086.	5.8	95
385	2D WS2 nanosheet supported Pt nanoparticles for enhanced hydrogen evolution reaction. International Journal of Hydrogen Energy, 2017, 42, 5472-5477.	3.8	45
386	Synthesis of thickness-controlled cuboid WO3 nanosheets and their exposed facets-dependent acetone sensing properties. Journal of Alloys and Compounds, 2017, 696, 490-497.	2.8	58
387	H2-Ar dilution for improved c-Si quantum dots in P-doped SiNx:H thin film matrix. Applied Surface Science, 2017, 396, 235-242.	3.1	3
388	Synthesis of Ag quantum dots sensitized WO3 nanosheets and their enhanced acetone sensing properties. Materials Letters, 2017, 186, 66-69.	1.3	45
389	Modeling of triangular-shaped substrates for light trapping in microcrystalline silicon solar cells. Optics Communications, 2017, 383, 304-309.	1.0	5
390	Ag Nanoparticle Enhanced Flexible Thin-Film Silicon Solar Cells. Journal of Nanoscience and Nanotechnology, 2017, 17, 3689-3694.	0.9	2
391	Optical Properties of Multilayered Ge Nanocrystals Embedded in SiO <i><sub>x</sub></i> GeN <i><sub>y</sub></i> Thin Films. Journal of Nanoscience and Nanotechnology, 2017, 17, 3519-3522.	0.9	0
392	Telluriumâ€Assisted Epitaxial Growth of Largeâ€Area, Highly Crystalline ReS <sub>2</sub> Atomic Layers on Mica Substrate. Advanced Materials, 2016, 28, 5019-5024.	11.1	169
393	Intrinsic Raman signatures of pristine hybrid perovskite CH <sub>3</sub> NH <sub>3</sub> PbI <sub>3</sub> and its multiple stages of structure transformation. , 2016, , .		0
394	Controlled Pt Monolayer Fabrication on Complex Carbon Fiber Structures for Superior Catalytic Applications. Electrochimica Acta, 2016, 222, 1522-1527.	2.6	9
395	Photoinduced surface voltage mapping study for large perovskite single crystals. Applied Physics Letters, 2016, 108, 181604.	1.5	13
396	Band alignment of TiO2/FTO interface determined by X-ray photoelectron spectroscopy: Effect of annealing. AIP Advances, 2016, 6, .	0.6	17

#	Article	IF	CITATIONS
397	Optical and electrical properties of high-quality Ti2O3 epitaxial film grown on sapphire substrate. Applied Physics A: Materials Science and Processing, 2016, 122, 1.	1.1	10
398	Stable high efficiency perovskite solar cells using vacuum deposition. , 2016, , .		0
399	Influence of oxygen pressure on the structural and electrical properties of CuO thin films prepared by pulsed laser deposition. Materials Letters, 2016, 176, 282-284.	1.3	36
400	Fabrication of a Cu2MnSn(S,Se)4thin film based on a low-cost degradable solution process. CrystEngComm, 2016, 18, 4744-4748.	1.3	5
401	Kesterite Cu <sub>2</sub> Zn(Sn,Ge)(S,Se) <sub>4</sub> thin film with controlled Ge-doping for photovoltaic application. Nanoscale, 2016, 8, 10160-10165.	2.8	31
402	One-pot hydrothermal fabrication of layered Î <sup>2</sup> -Ni(OH) 2 /g-C 3 N 4 nanohybrids for enhanced photocatalytic water splitting. Applied Catalysis B: Environmental, 2016, 194, 74-83.	10.8	102
403	Multiple-Stage Structure Transformation of Organic-Inorganic Hybrid Perovskite <mml:math xmlns:mml="http://www.w3.org/1998/Math/MathML" display="inline"&gt;<mml:mrow><mml:msub><mml:mrow><mml:mi>CH</mml:mi></mml:mrow><mml:mrow><mm Physical Review X, 2016, 6, .</mm </mml:mrow></mml:msub></mml:mrow></mml:math 	l:mn8>3 <th>nml:mn&gt;</th>	nml:mn>
404	20â€mmâ€Large Singleâ€Crystalline Formamidiniumâ€Perovskite Wafer for Mass Production of Integrated Photodetectors. Advanced Optical Materials, 2016, 4, 1829-1837.	3.6	316
405	Thinness―and Shapeâ€Controlled Growth for Ultrathin Singleâ€Crystalline Perovskite Wafers for Mass Production of Superior Photoelectronic Devices. Advanced Materials, 2016, 28, 9204-9209.	11.1	296
406	Flowerlike Cu <sub>2</sub> Te architectures constructed from ultrathin nanoflakes as superior dye adsorbents for wastewater treatment. RSC Advances, 2016, 6, 79612-79619.	1.7	9
407	Surface optimization to eliminate hysteresis for record efficiency planar perovskite solar cells. Energy and Environmental Science, 2016, 9, 3071-3078.	15.6	870
408	Superior adsorption performance for triphenylmethane dyes on 3D architectures assembled by ZnO nanosheets as thin as â^1⁄41.5 nm. Journal of Hazardous Materials, 2016, 318, 732-741.	6.5	51
409	Highly stabilized perovskite solar cell prepared using vacuum deposition. RSC Advances, 2016, 6, 93525-93531.	1.7	10
410	Perovskite CH <sub>3</sub> NH <sub>3</sub> Pb(Br <sub>x</sub> I <sub>1â^'x</sub> ) <sub>3</sub> single crystals with controlled composition for fine-tuned bandgap towards optimized optoelectronic applications. Journal of Materials Chemistry C, 2016, 4, 9172-9178.	2.7	120
411	Improved PEDOT:PSS/c-Si hybrid solar cell using inverted structure and effective passivation. Scientific Reports, 2016, 6, 35091.	1.6	60
412	Hysteresisâ€Suppressed Highâ€Efficiency Flexible Perovskite Solar Cells Using Solidâ€State Ionicâ€Liquids for Effective Electron Transport. Advanced Materials, 2016, 28, 5206-5213.	11.1	387
413	Effective solvent-additive enhanced crystallization and coverage of absorber layers for high efficiency formamidinium perovskite solar cells. RSC Advances, 2016, 6, 56807-56811.	1.7	25
414	AFORS-HET simulation study of HIT solar cells: Significance of inversion layer 2016		1

414 AFORS-HET simulation study of HIT solar cells: Significance of inversion layer. , 2016, , .

#	Article	IF	CITATIONS
415	One-pot fabrication of NiFe 2 O 4 nanoparticles on α-Ni(OH) 2 nanosheet for enhanced water oxidation. Journal of Power Sources, 2016, 324, 499-508.	4.0	57
416	Perovskite/germanium tandem: A potential high efficiency thin film solar cell design. Optics Communications, 2016, 380, 1-5.	1.0	20
417	Ag Nanoparticle-Sensitized WO <sub>3</sub> Hollow Nanosphere for Localized Surface Plasmon Enhanced Gas Sensors. ACS Applied Materials & Interfaces, 2016, 8, 18165-18172.	4.0	90
418	The effect of transparent conductive oxide on the performance CH3NH3PbI3 perovskite solar cell without electron/hole selective layers. Solar Energy, 2016, 135, 654-661.	2.9	27
419	Solarâ€toâ€Hydrogen Efficiency of 9.5 % by using a Thinâ€Layer Platinum Catalyst and Commercial Amorphous Silicon Solar Cells. ChemCatChem, 2016, 8, 1713-1717.	1.8	7
420	Modulating crystal grain size and optoelectronic properties of perovskite films for solar cells by reaction temperature. Nanoscale, 2016, 8, 3816-3822.	2.8	179
421	Superior texture-controlled ZnO thin film using electrochemical deposition. Solar Energy, 2016, 125, 192-197.	2.9	12
422	Color-Tuned Perovskite Films Prepared for Efficient Solar Cell Applications. Journal of Physical Chemistry C, 2016, 120, 42-47.	1.5	106
423	2D-MoO <sub>3</sub> nanosheets for superior gas sensors. Nanoscale, 2016, 8, 8696-8703.	2.8	156
424	Fabrication of TiO2/C3N4 heterostructure for enhanced photocatalytic Z-scheme overall water splitting. Applied Catalysis B: Environmental, 2016, 191, 130-137.	10.8	344
425	Controlled electrodeposition of Au monolayer film on ionic liquid. Applied Surface Science, 2016, 371, 258-261.	3.1	3
426	The effects of Ag particle morphology on the antireflective properties of silicon textured using Ag-assisted chemical etching. Journal of Alloys and Compounds, 2016, 670, 156-160.	2.8	8
427	Heterojunction CuO@ZnO microcubes for superior p-type gas sensor application. Journal of Alloys and Compounds, 2016, 672, 374-379.	2.8	67
428	Au nanoparticle enhanced thin-film silicon solar cells. Solar Energy Materials and Solar Cells, 2016, 147, 225-234.	3.0	24
429	Synthesis of CuO microstructures with controlled shape and size and their exposed facets induced enhanced ethanol sensing performance. Sensors and Actuators B: Chemical, 2016, 227, 328-335.	4.0	35
430	MoS 2 /sulfur and nitrogen co-doped reduced graphene oxide nanocomposite for enhanced electrocatalytic hydrogen evolution. International Journal of Hydrogen Energy, 2016, 41, 916-923.	3.8	40
431	Effect of nanopits size and spacing on the light absorption in silicon thin film solar cells. Optik, 2016, 127, 1003-1006.	1.4	0
432	Ag nanoparticle enhanced light trapping in hydrogenated amorphous silicon germanium solar cells on flexible stainless steel substrate. Solar Energy Materials and Solar Cells, 2016, 144, 63-67.	3.0	22

#	Article	IF	CITATIONS
433	Responses of three-dimensional porous ZnO foam structures to the trace level of triethylamine and ethanol. Sensors and Actuators B: Chemical, 2016, 223, 650-657.	4.0	39
434	Perovskite as an effective V oc switcher for high efficiency polymer solar cells. Nano Energy, 2016, 20, 126-133.	8.2	22
435	Enhancing the Performance of Amorphous‣ilicon Photoanodes for Photoelectrocatalytic Water Oxidation. ChemSusChem, 2015, 8, 3987-3991.	3.6	17
436	Twoâ€Inchâ€Sized Perovskite CH <sub>3</sub> NH <sub>3</sub> PbX <sub>3</sub> (X = Cl, Br, I) Crystals: Growth and Characterization. Advanced Materials, 2015, 27, 5176-5183.	11.1	914
437	The Photoluminescence Behaviors of a Novel Reddish Orange Emitting Phosphor Caln <sub>2</sub> O <sub>4</sub> :Sm <sup>3+</sup> Codoped with Zn <sup>2+</sup> or Al <sup>3+</sup> lons. Journal of Nanomaterials, 2015, 2015, 1-5.	1.5	3
438	An up-scalable approach to CH3NH3PbI3 compact films for high-performance perovskite solar cells. Nano Energy, 2015, 15, 670-678.	8.2	79
439	p-Layer bandgap engineering for high efficiency thin film silicon solar cells. Materials Science in Semiconductor Processing, 2015, 39, 192-199.	1.9	15
440	Effective strategy for stabilized perovskite solar cells using tandem architecture. , 2015, , .		0
441	Superior photocatalytic activities of NiO octahedrons with loaded AgCl particles and charge separation between polar NiO {111} surfaces. Applied Catalysis B: Environmental, 2015, 172-173, 165-173.	10.8	41
442	Fabrication gallium/graphene core–shell nanoparticles by pulsed laser deposition and their applications in surface enhanced Raman scattering. Materials Letters, 2015, 143, 194-196.	1.3	13
443	Li doping effect on the photoluminescence behaviors of KSrPO4:Dy3+ phosphors for WLED light. Materials Research Bulletin, 2015, 64, 364-369.	2.7	34
444	Composition controlled preparation of Cu–Zn–Sn precursor films for Cu2ZnSnS4 solar cells using pulsed electrodeposition. Journal of Alloys and Compounds, 2015, 650, 1-7.	2.8	32
445	Effective light trapping by hybrid nanostructure for crystalline silicon solar cells. Solar Energy Materials and Solar Cells, 2015, 140, 180-186.	3.0	36
446	One-step preparation of optically transparent Ni-Fe oxide film electrocatalyst for oxygen evolution reaction. Electrochimica Acta, 2015, 169, 402-408.	2.6	46
447	Visible-light photocatalysis in Cu <sub>2</sub> Se nanowires with exposed {111} facets and charge separation between (111) and (11,,11,,11,) polar surfaces. Physical Chemistry Chemical Physics, 2015, 17, 13280-13289.	1.3	42
448	One-step hydrothermal synthesis of monolayer MoS <sub>2</sub> quantum dots for highly efficient electrocatalytic hydrogen evolution. Journal of Materials Chemistry A, 2015, 3, 10693-10697.	5.2	320
449	Alternating precursor layer deposition for highly stable perovskite films towards efficient solar cells using vacuum deposition. Journal of Materials Chemistry A, 2015, 3, 9401-9405.	5.2	146
450	Controllable synthesis of silicon nano-particles using a one-step PECVD-ionic liquid strategy. Journal of Materials Chemistry A, 2015, 3, 10233-10237.	5.2	0

#	Article	IF	CITATIONS
451	High efficiency flexible perovskite solar cells using superior low temperature TiO <sub>2</sub> . Energy and Environmental Science, 2015, 8, 3208-3214.	15.6	519
452	Pt monolayer coating on complex network substrate with high catalytic activity for the hydrogen evolution reaction. Science Advances, 2015, 1, e1400268.	4.7	97
453	Lateral matching of periodic front and back textures in thin film silicon solar cells. Optics Communications, 2015, 357, 28-33.	1.0	2
454	Facile synthesis of an iron doped rutile TiO <sub>2</sub> photocatalyst for enhanced visible-light-driven water oxidation. Journal of Materials Chemistry A, 2015, 3, 21434-21438.	5.2	50
455	A Se-doped MoS <sub>2</sub> nanosheet for improved hydrogen evolution reaction. Chemical Communications, 2015, 51, 15997-16000.	2.2	167
456	Synthesis of hierarchical structure Cu2SnSe3 microsphere by a solvothermal method. Materials Letters, 2015, 161, 727-730.	1.3	4
457	Controlled ZnO hierarchical structure for improved gas sensing performance. Sensors and Actuators B: Chemical, 2015, 209, 343-351.	4.0	31
458	Topology and texture controlled ZnO thin film electrodeposition for superior solar cell efficiency. Solar Energy Materials and Solar Cells, 2015, 134, 54-59.	3.0	40
459	Superior sensor performance from Ag@WO3 core–shell nanostructure. Journal of Alloys and Compounds, 2015, 623, 127-131.	2.8	34
460	One-pot synthesis of Co-doped ZnO hierarchical aggregate and its high gas sensor performance. Materials Chemistry and Physics, 2015, 149-150, 344-349.	2.0	22
461	Effect of Ag Film Thickness on the Morphology and Light Scattering Properties of Ag Nanoparticles. Nanoscience and Nanotechnology Letters, 2014, 6, 392-397.	0.4	4
462	InOCl nanosheets with exposed {001} facets: Synthesis, electronic structure and surprisingly high photocatalytic activity. Applied Catalysis B: Environmental, 2014, 152-153, 390-396.	10.8	13
463	Millimeter-long multilayer graphene nanoribbons prepared by wet chemical processing. Carbon, 2014, 71, 120-126.	5.4	14
464	Direct growth of ZnO nanodisk networks with an exposed (0001) facet on Au comb-shaped interdigitating electrodes and the enhanced gas-sensing property of polar {0001} surfaces. Sensors and Actuators B: Chemical, 2014, 195, 71-79.	4.0	59
465	Diameter regulated ZnO nanorod synthesis and its application in gas sensor optimization. Journal of Alloys and Compounds, 2014, 586, 436-440.	2.8	26
466	Preparation of ZnO hollow spheres with different surface roughness and their enhanced gas sensing property. Sensors and Actuators B: Chemical, 2014, 197, 58-65.	4.0	68
467	Graphene oxide – a surprisingly good nucleation seed and adhesion promotion agent for one-step ZnO lithography and optoelectronic applications. Journal of Materials Chemistry C, 2014, 2, 8956-8961.	2.7	24
468	Size-dependent optical properties and enhanced visible light photocatalytic activity of wurtzite CdSe hexagonal nanoflakes with dominant {001} facets. Journal of Alloys and Compounds, 2014, 610, 62-68.	2.8	16

#	Article	IF	CITATIONS
469	Synthesis and formation mechanism of flowerlike architectures assembled from ultrathin NiO nanoflakes and their adsorption to malachite green and acid red in water. Chemical Engineering Journal, 2014, 239, 141-148.	6.6	71
470	Agx@WO3 core-shell nanostructure for LSP enhanced chemical sensors. Scientific Reports, 2014, 4, 6745.	1.6	116
471	Fabrication and Light Scattering Properties of Size Controlled Aluminum Surface Periodic Nanopits. Nanoscience and Nanotechnology Letters, 2014, 6, 470-476.	0.4	2
472	Development of an alcohol sensor based on ZnO nanorods synthesized using a scalable solvothermal method. Sensors and Actuators B: Chemical, 2013, 185, 735-742.	4.0	44
473	Generation and manipulation of higher order Fano resonances in plasmonic nanodisks with a built-in missing sectorial slice. Europhysics Letters, 2013, 104, 47009.	0.7	6
474	12.0% Efficiency on large area, encapsulated, multijunction nc-Si:H based solar cells. , 2011, , .		3
475	Hydrazide Derivatives for Defect Passivation in Pure CsPbI3 Perovskite Solar Cells. Angewandte Chemie, 0, , .	1.6	4